INTERNATIONAL JOURNAL OF ADAPTIVE CONTROL AND SIGNAL PROCESSING
Int. J. Adapt. Control Signal Process. 2007; **21**:375–390
Published online 18 October 2006 in Wiley InterScience (www.interscience.wiley.com). DOI: 10.1002/acs.927

Detection and clustering of light charged particles via system-identification techniques

F. Previdi[1,4,*,†], Sergio M. Savaresi[2], P. Guazzoni[3,4] and L. Zetta[3,4]

[1] *Dipartimento di Ingegneria Gestionale e dell'Informazione, Università degli Studi di Bergamo, Italy*
[2] *Dipartimento di Elettronica ed Informazione, Politecnico di Milano, Italy*
[3] *Dipartimento di Fisica, Università degli Studi di Milano, Italy*
[4] *Istituto Nazionale di Fisica Nucleare, Milano, Italy*

SUMMARY

The problem considered in this work is the classification of the particles produced by the collision of a heavy ion beam on a target. Each particle is captured by a detector and results in a signal (which is the impulse response of a dynamic linear system), which is measured by a digital acquisition system. The assumption made herein is that the shape of the impulse-response contains complete information on the particle, and the classification can be done by pulse-shape, analysis.

In this work, a complete procedure for the particle identification is proposed. The main idea is to use the cascade of a state-space identification algorithm and a parametric non-linear map using the model parameters as input regressors. The algorithm has been tested on a large set of impulse-responses and provides a fully automatic accurate classification of the isotopes.

This work focuses on isotopic identification of the most energetic light charged particles (LCP). All the experiments are made with the large detector array CHIMERA (Charge Heavy Ions Mass and Energy Resolving Array).

Received 30 September 2005; Revised 10 April 2006; Accepted 11 April 2006

KEY WORDS: heavy ion reaction physics; impulse response; state-space identification; classification; non-linear maps

1. INTRODUCTION AND PROBLEM STATEMENT

The topic of this paper is a classical problem in nuclear physics: the classification of the particles produced by the nucleus–nucleus collision.

*Correspondence to: F. Previdi, Dipartimento di Ingegneria Gestionale e dell'Informazione, Università degli Studi di Bergamo, Via Marconi, 5, Dalmine (Bergamo) 24044, Italy.
† E-mail: previdi@unibg.it

Contract/grant sponsor: MIUR project

The standard investigation approach in heavy ion reaction physics is the measurement and analysis of the collision effects of a heavy ion beam over a target. The nuclear reactions induced by the nucleus–nucleus collision produce a large number of fragments with different energy, charge and mass values. These fragments move away from the collision point in 4π directions (i.e. in all directions), and are captured by large detector arrays [1].

The specific detector considered in this work is the large detector array CHIMERA (charge heavy ions mass and energy resolving array). Each detection cell of CHIMERA contains two main elements: a thin *Si detector* and a thick *CsI*(*Tl*) *scintillation counter* read out by a photodiode. The Si detector is a semiconductor device in which the impact of a charged particle produces a charge displacement, which is detected as a current by means of an applied voltage. The CsI(Tl) scintillator is a solid-state detector, which generates a light pulse when hit by a charged particle.

The detection path of CHIMERA is concisely described in Figure 1. When a reaction product hits the detector, it loses a fraction of its energy (ΔE) in the Si detector and the remaining part (E) in the CsI(Tl) scintillator. The energy released in the scintillator is transformed into a light pulse collected by a photodiode. Then, the output of the photodiode is fed into a preamplification stage and a signal $v(t)$ is generated. Similarly, the output of the Si detector is fed into a preamplifier and a signal $u(t)$ is generated, from which the energy loss ΔE can be measured. The residual energy E can be measured using $v(t)$.

Starting from these measurements, the problem is to correctly classify the corresponding particle.

The classical method for the classification of the fragments produced by nuclear reactions at intermediate energy is generally based on manual or semi-automatic procedures [2]. In Figure 2 a zoom of a typical E–ΔE scatter plot is displayed, for a set of elements ranging from hydrogen (charge $Z = 1$) to beryllium (charge $Z = 4$). It is easy to see that good isotopic identification is obtained for heavy charged particles (HCPs, $Z \geqslant 3$) in the E–ΔE scatter plot, whereas in the case of light charged particles (LCPs, $Z < 3$) a good isotopic identification is possible only for less energetic products.

The classification of LCP henceforth requires the inspection of the complete impulse CsI(Tl) response $v(t)$, which is the most informative measurement. This technique is known in literature as pulse-shape analysis, and it is grounded on the idea that different particles interact with the detector in different ways, and the shape of the pulse response represents a complete signature (mass, charge and energy) of the particle. In Figure 3 an example of measured impulse response $v(t)$ is displayed.

Pulse-shape analysis is described in the literature, and it has been widely adopted [3–14]. It usually consists in a rough estimation of two parameters (which are somehow related to the two main time constants of the impulse response—see, e.g. [4,6,14] and an analysis of their value for

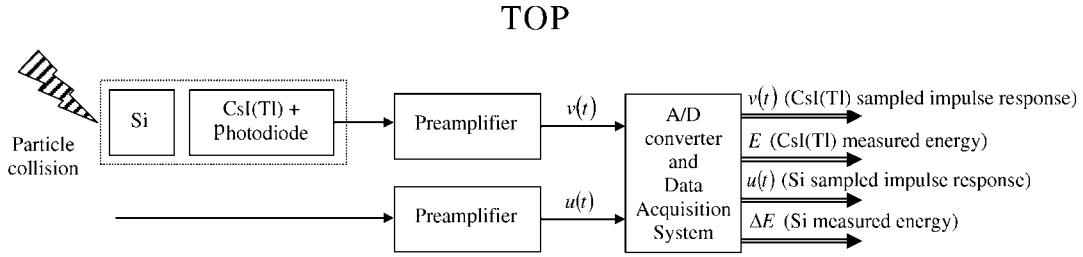

Figure 1. Layout of the measurement path.

DOI: 10.1002/acs

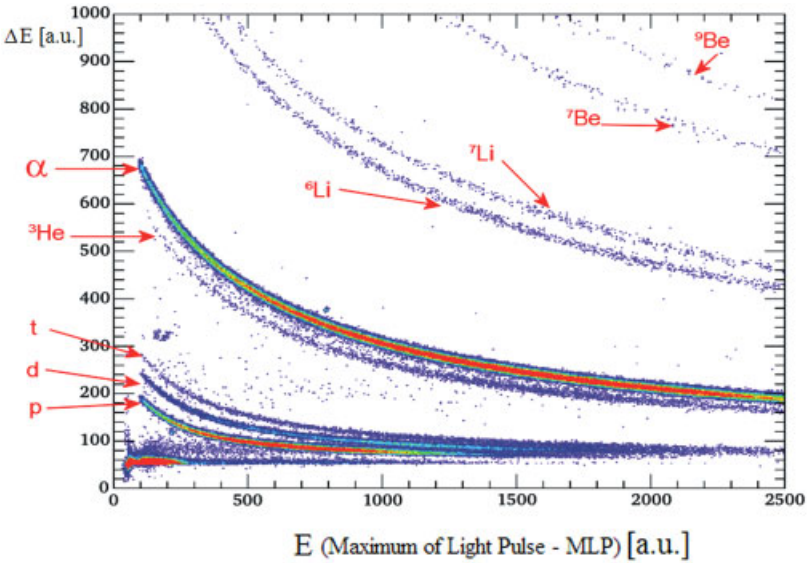

Figure 2. Example of a E–ΔE scatter plot for a beam of ^{20}Ne at 21 MeV per nucleon on a ^{12}C target. This picture is a zoom of the whole plot and it concerns only the lighter fragments.

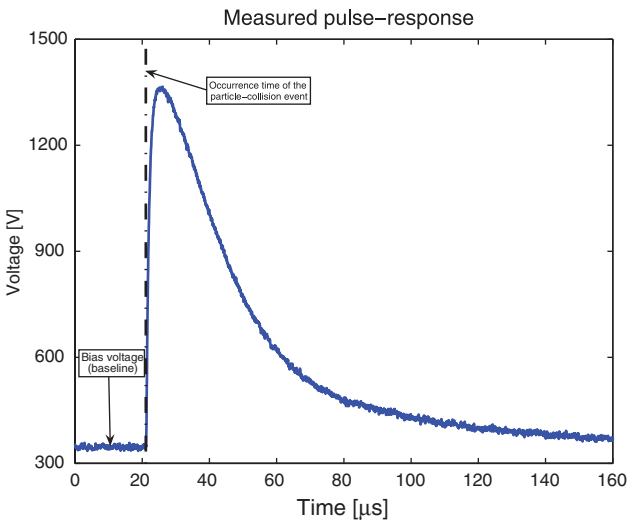

Figure 3. An example of measured CsI(Tl) impulse response $v(t)$.

particle classification. The objective of this work is to develop a complete, more accurate, and fully automatic analysis of the impulse response, using system-identification tools. More specifically, the method proposed herein is based on a two-step algorithm:

- a subspace identification method is used to estimate the four parameters of a discrete-time linear model from the sampled impulse response [15–18];

DOI: 10.1002/acs

- a parametric non-linear map is identified; its output is the particle classification; its input regressor vector is the set of parameters of the estimated dynamic linear model [19].

The tuning and the validation of the algorithm have been performed using a set of pulses produced by known particles, in an experiment where a beam of ^{20}Ne at 21 MeV per nucleon bombards a ^{12}C target.

The development of the proposed classification method has been made possible by the introduction of the new digital electronic equipment, recently developed using CHIMERA detectors, which allow fast digital sampling of the measured pulses [20].

The paper is organized as follows: in Section 2 the experimental set-up is outlined. In Section 3 the state-space identification of dynamic models from impulse response is described, and the experimental results are outlined. In Section 4 the particle classification is presented and discussed.

2. EXPERIMENTAL SET-UP

The experimental device used for this work is the 4π multidetector array CHIMERA installed at Laboratori Nazionali del Sud (Catania, Italy), which is specifically designed for the study of heavy ion reactions at intermediate energy (up to 100 MeV/nucleon). Its aim is the detection of the products of a nuclear reaction between heavy ions. In this context, detection means the measurement of the energy, mass and charge of each fragment. The 4π attribute means that the detector is composed of many detection modules which almost completely cover the solid angle. CHIMERA is able to intercept almost all the fragments produced in a nuclear reaction, whatever is their direction of arrival. CHIMERA is specifically designed to investigate fundamental heavy ion nuclear physics at intermediate energies, including, as a possible result of nuclear reactions, the nuclear matter equation of state, the liquid–vapour phase transitions, the hot nuclei instability, the ion–ion collision dynamics and the multifragmentation (which is the phenomenon this work focuses on).

During CHIMERA standard operating conditions, a beam of accelerated nuclei delivered by a superconducting cyclotron is shot over a thin target placed inside a vacuum chamber. When an accelerated nucleus collides over a target nucleus, the hot and compressed system formed in the early stage of the collision can de-excite, leading to the generation of many fragments with different charge, mass and energy, ranging from a single proton to the beam element and moving away from the collision point in 4π directions. The fragments are distributed on a wide energy range, whose extreme values depend on the incident beam energy and the occurred reaction.

CHIMERA is constituted by a set of 1192 detection cells arranged in 35 rings with cylindrical geometry around the beam axis (Figure 4). The rings are divided into two blocks. The first block is a set of 18 rings, composed of 688 detectors, arranged with a cylindrical geometry. They are placed at a distance from the target along the beam direction variable from 3.5 to 1.0 m, with increasing angle. This first block covers the polar angle between 1° and 30°. The second block is a set of 17 rings, composed of 504 detectors, placed around the target with a 0.4 m radius spherical geometry inside the reaction vacuum chamber. They cover the polar angle ranging between 30° and 176°. Using this set-up, about 94% of 4π is covered.

DOI: 10.1002/acs

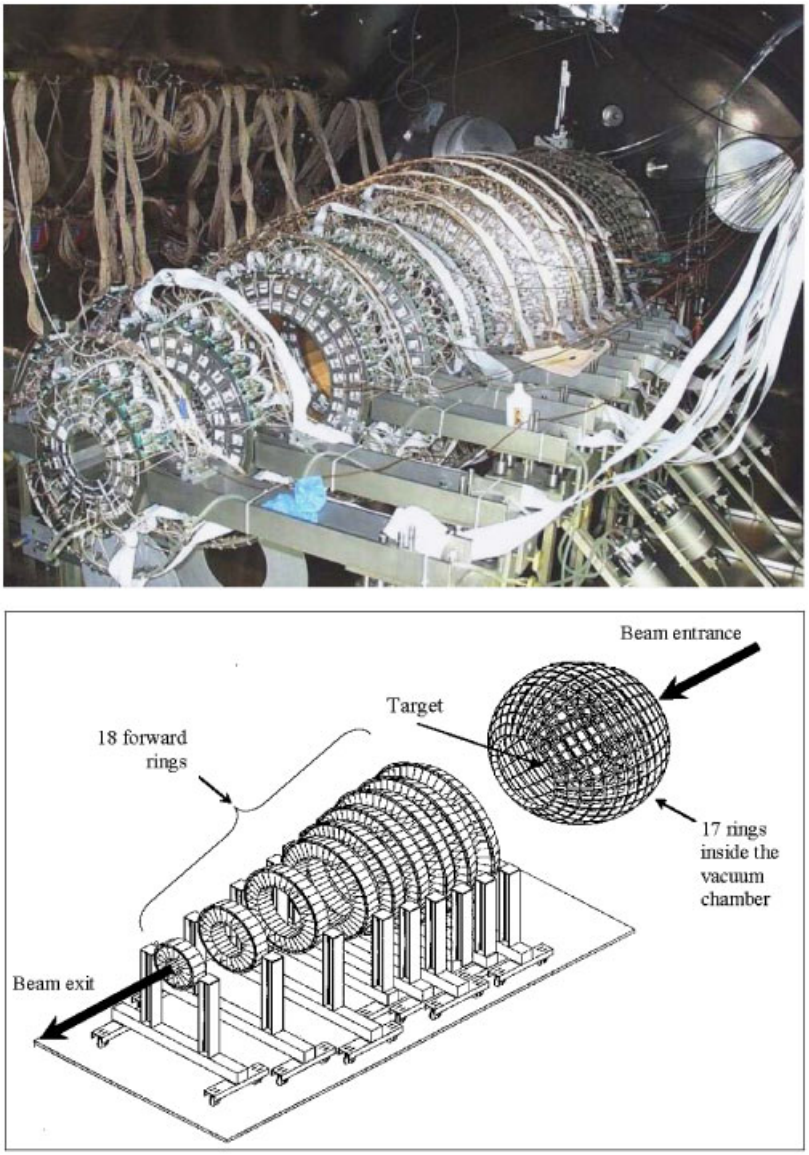

Figure 4. An image (top) and a schematic representation (bottom) of CHIMERA.

Each detection cell is a telescope composed of a CsI(Tl) scintillation crystal with a thin Si detector in front of it. After the beam collision over the target, the particles produced by the reaction move towards the detection cells. When a particle enters a telescope, it travels through the Si detector, releasing a fraction ΔE of its energy, which is measured by the detector; then, it goes forward inside the scintillator, which is supposed to be thick enough so that the particle comes to a complete stop and releases the remaining part E of its initial energy.

DOI: 10.1002/acs

Table I. Description of the data set.

Isotope	Atomic number (Z)	Atomic mass number (A)	Number of available pulses
^{1}H (protons)	1	1	921
^{2}H (deuterons)	1	2	981
^{3}H (tritons)	1	3	992
^{3}He	2	3	988
^{4}He	2	4	977
^{6}Li	3	6	992
^{7}Li	3	7	900
^{7}Be	4	7	512
^{9}Be	4	9	530
Heavy ions	$\geqslant 5$	$\geqslant 10$	991

In the scintillation counter, the energy delivered by the particle is converted into a light pulse [21,22]. The scintillator is coupled to a photodiode, which collects the emitted light and produces a current output, strictly proportional to the light intensity. The current is transformed into a measurable voltage signal $v(t)$ by means of a charge preamplifier. The voltage pulse is sampled with 10 ns sampling time and 14-bit resolution. For each pulse, 2048 samples are measured and stored in the system memory. A full description of the digital measurement set-up can be found in [5].

The data set used in this work has been collected during an experimental session involving a beam of ^{20}Ne at 21 MeV per nucleon on a ^{12}C target and concerns only the pulses from the CsI(Tl) scintillators. The data set consists of 8784 pulses, each composed of 2048 samples measured with a 10 ns sampling time and about 20 μs long. After the elimination of the baseline, each pulse is composed of about 1600 samples. The data set is described in Table I. Note that the pulses have been preliminarily classified using the standard two-gate method [20]. The two-gate method is based on the comparison between the so-called fast and slow components of the light pulse. The estimates of the two components are obtained by integrating, over two time intervals Δt_1 and Δt_2, the output of the shaping amplifier at two proper time t_1 and t_2.

3. SYSTEM IDENTIFICATION FROM IMPULSE RESPONSES

For each particle from the CsI(Tl), a 16 μs long impulse response $v(t)$ is measured. The basic idea of the method proposed in this work is to consider the measured signal $v(t)$ as the impulse response of a SISO (single input single output) linear time-invariant dynamic system and to solve a system-identification problem. The estimated parameters of the dynamic system are then used as input regressors of a parametric non-linear map which performs the particle classification.

More specifically, it is assumed that $v(t)$ is the impulse response of a third-order linear system, and that its Laplace transform $V(s)$ has the following form (see Figure 5):

$$V(s) = \frac{1}{1 + s\tau_{\mathrm{m}}}\left(\frac{\mu_{\mathrm{s}}}{1 + s\tau_{\mathrm{s}}} + \frac{\mu_{\mathrm{f}}}{1 + s\tau_{\mathrm{f}}}\right) \tag{1}$$

DOI: 10.1002/acs

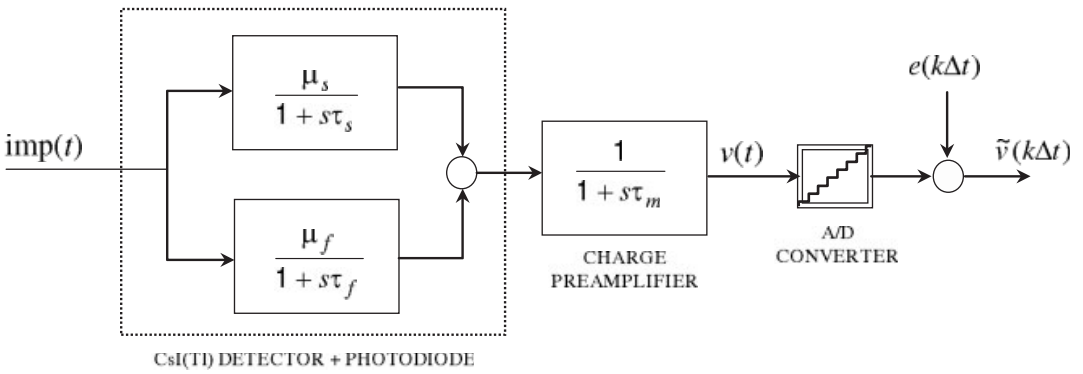

Figure 5. Sketch of the model and the measurement process.

As a matter of fact, it is assumed that [4–6,14,20]:

- the dynamics of the particle interaction with the detector can be modelled as a four-parameter second-order strictly proper (single-zero) linear system with a fast pole (time constant τ_f) and a slow pole (time constant τ_s);
- the dynamic effect of the charge preamplifier can be modelled as a unitary-gain first-order low-pass filter (time constant τ_m).

Since the data acquisition is made with a digital system, the measurement device is complemented with an A/D converter (sampling time 10 ns, 14-bit resolution). Moreover, the signal is assumed to be affected by a stationary zero-mean additive noise, namely,

$$\tilde{v}(k\Delta T) = v(k\Delta T) + e(k\Delta T), \quad k = 1, 2, 3, 4, \ldots, N \tag{2}$$

where:

- ΔT is the sampling time, k is the discrete-time index and N is the available number of data ($N = 1600$);
- $\tilde{v}(k\Delta T)$ is the measured (noisy) impulse response;
- $v(k\Delta T)$ is the noise-free impulse response;
- $e(k\Delta T)$ is the measurement noise (which also embeds the un-modelled dynamics);

(in the rest of the paper the notation will be simplified by dropping the term ΔT).

When impulse response measurements are available, it is possible to give a state-space realization of the system by resorting to the Ho–Kalman framework [23–26]. The method is now briefly recalled.

Consider the following state-space representation of a strictly proper discrete-time SISO linear system:

$$\begin{aligned} x(k+1) &= Ax(k) + Bu(k) \\ y(t) &= Cx(k) \end{aligned} \tag{3}$$

where $x(t) \in \Re^n$, $u(t) \in \Re$ and $y(t) \in \Re$ are the system state, input and output, respectively.

DOI: 10.1002/acs

Suppose that N noisy measurements of the impulse response (Markov parameters) of the system are available

$$\tilde{v}(k) = v(k) + e(k), \quad k = 1, 2, \ldots, N \tag{4}$$

The identification problem is to find the set of matrices $\{A, B, C\}$ which represents a minimum-order realization of the system.

This problem can be solved with the following five-step procedure [15–18, 22, 24, 26].

- Using the impulse response measurements, build the following Hankel matrix with i rows and j columns:

$$\tilde{H}_{ij} = \begin{bmatrix} \tilde{v}(1) & \tilde{v}(2) & \cdots & \cdots & \tilde{v}(j) \\ \tilde{v}(2) & \tilde{v}(3) & \cdots & \cdots & \tilde{v}(j+1) \\ \vdots & \vdots & \cdots & \cdots & \vdots \\ \vdots & \vdots & \cdots & \cdots & \vdots \\ \tilde{v}(i) & \tilde{v}(i+1) & \cdots & \cdots & \tilde{v}(i+j-1) \end{bmatrix} \tag{5}$$

  where i, j are user-defined parameters such that $i + j - 1 = N$ (usually, $i, j \gg n$—see [27] for a discussion on the issue of selecting these parameters).
- Compute the SVD of $\tilde{H}_{ij}$ [28]:

$$\tilde{H}_{ij} = USV^{\mathrm{T}} \tag{6}$$

  where $U = [u_1, \ldots, u_i] \in \Re^{i \times i}$ and $V = [v_1, \ldots, v_j] \in \Re^{j \times j}$ are two orthogonal matrices, being $\{u_l\}_{l=1,\ldots,i}$ and $\{v_l\}_{l=1,\ldots,j}$ the column vectors of U and V, respectively; $S = \mathrm{diag}(\sigma_1, \ldots, \sigma_p) \in \Re^{i \times j}$, with $p = \min\{i, j\}$, and $\sigma_1 \geqslant \sigma_2 \geqslant \cdots \geqslant \sigma_p \geqslant 0$.
- Compute the reduced-order Hankel matrix. Choose a value for n (the order of the system, so that $n \leqslant p$), and partition the matrices U, S, V as follows:

$$U = [U_S \;\; U_N], \quad S = \begin{bmatrix} S_S & 0 \\ 0 & S_N \end{bmatrix}, \quad V = [V_S \;\; V_N]$$

$$U_S = [u_1, \ldots, u_n] \in \Re^{i \times n}, \quad U_N = [u_{n+1}, \ldots, u_i] \in \Re^{i \times (i-n)}$$

$$V_S = [v_1, \ldots, v_n] \in \Re^{j \times n}, \quad V_N = [v_{n+1}, \ldots, v_j] \in \Re^{j \times (j-n)}$$

$$S_S = \mathrm{diag}(\sigma_1, \ldots, \sigma_n) \in \Re^{n \times n}, \quad S_N \in \Re^{(j-n) \times (i-n)}$$

  By using the partitioned matrices, it is possible to write

$$\tilde{H}_{ij} = USV^{\mathrm{T}} = U_S S_S V_S^{\mathrm{T}} + U_N S_N V_N^{\mathrm{T}} \tag{7}$$

  The matrix $\tilde{H}_{ij,n} = U_S S_S V_S^{\mathrm{T}}$ is the reduced-order Hankel matrix of order n. The choice of the order n of the system can be performed by inspecting the magnitude of the singular values of the matrix S. In fact, it is usually possible to separate the set of the singular values

DOI: 10.1002/acs

into two subsets: the 'system' singular values and the 'noise' singular values. The elements of the first subset are expected to be significantly greater than the elements of the second subset. The cardinality of the first subset provides an estimate of n.

- Compute the matrices $\hat{\Gamma} = U_S S_S^{1/2}$ and $\hat{\Omega} = S_S^{1/2} V_S^{\mathrm{T}}$. These are estimates of the extended observability matrix and the extended reachability matrix, respectively.
- Compute the estimates of the system matrices as follows: $\hat{A} = (\hat{\Gamma}_{\uparrow})^{\dagger} \hat{\Gamma}_{\downarrow}$, where $\hat{\Gamma}_{\uparrow}$ and $\hat{\Gamma}_{\downarrow}$ are obtained from $\hat{\Gamma}$ deleting, respectively, the first row and last row; the symbol $\dagger$ indicates the matrix pseudoinverse operation; $\hat{B}$ is the first column of $\hat{\Omega}$; $\hat{C}$ is the first row of $\hat{\Gamma}$.

Once the estimated matrices $\{\hat{A}, \hat{B}, \hat{C}\}$ are available, the five parameters $\{\mu_s, \mu_f, \tau_s, \tau_f, \tau_m\}$ can be straightforwardly computed from $\{\hat{A}, \hat{B}, \hat{C}\}$.

The above identification procedure has been applied to each of the 8784 pulse responses available. The identification results are described in Figures 6–8.

In Figure 6, an example of estimated singular values (for one of the 8784 pulse responses) is displayed (very similar results are obtained for the other impulse responses). From Figure 6 one can clearly note that the order of the estimated dynamic system is $n = 3$. As a matter of fact the three 'signal' singular values are very clearly separated from the remaining 'noise' singular values. This confirms that the choice of model (1) is adequate.

In Figure 7 an example of measured and estimated impulse response is depicted. The fitting is extremely accurate (the two lines are almost indistinguishable). Again, this confirms that the selected model structure is adequate, and that the identification procedure works correctly.

Finally, in Figure 8 the whole set of the estimated values of the four parameters $\{\mu_s, \mu_f, \tau_s, \tau_f\}$ is displayed. It is interesting to see that the estimates of τ_f and the estimates of τ_s are in very good agreement with the values reported in the literature [4,6,14]. Also note that the parameter τ_m obviously does not depend on the type of particle; henceforth it is useless for particle classification; its estimated value is $\tau_m = 35.87\,\mu s$.

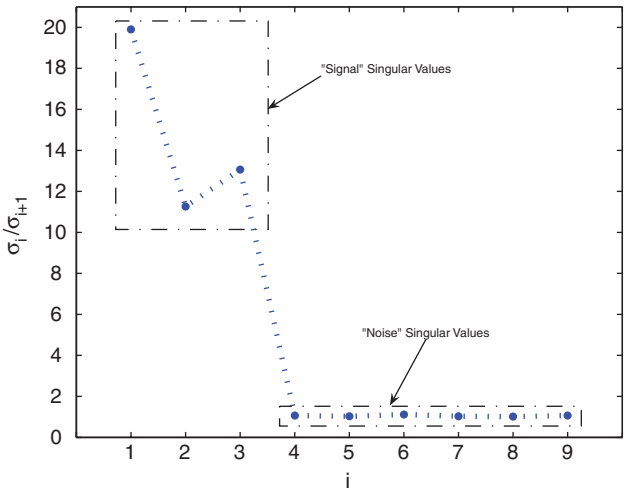

Figure 6. An example of singular values, estimated from impulse responses.

DOI: 10.1002/acs

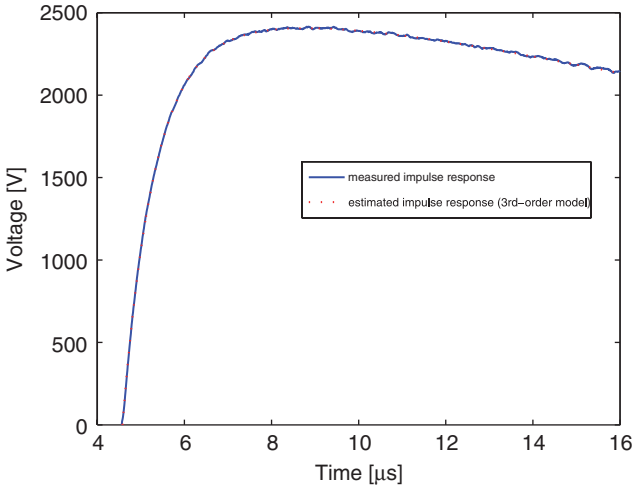

Figure 7. An example of measured and estimated impulse response.

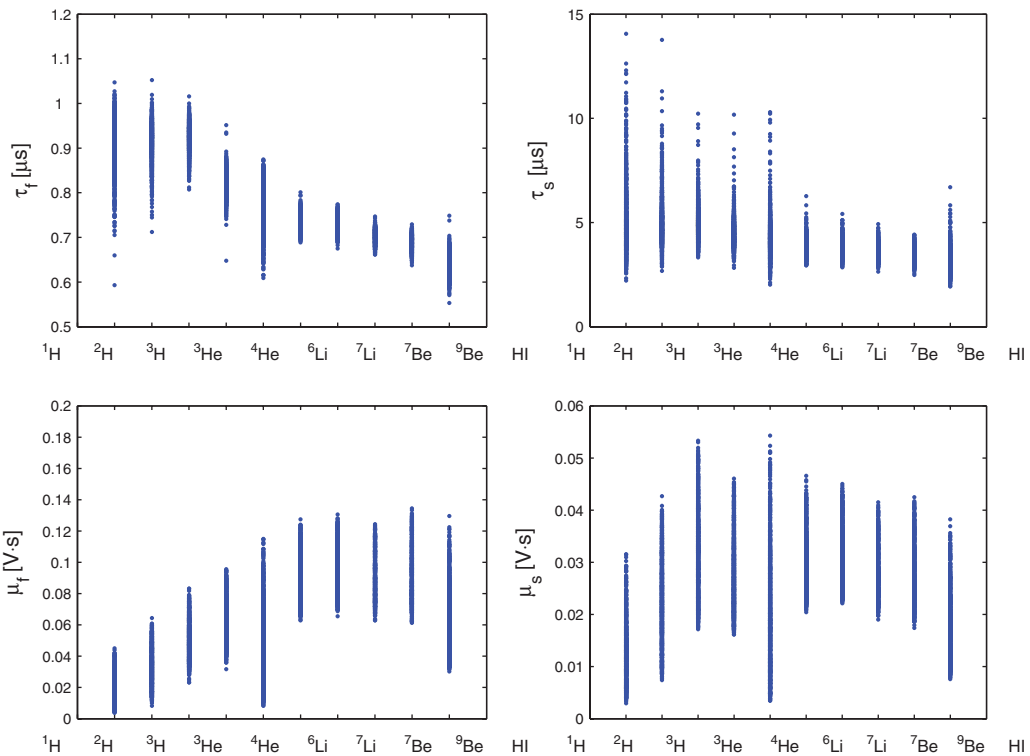

Figure 8. Estimated parameters $\{\mu_s, \mu_f, \tau_s, \tau_f\}$ for the 8784 pulse responses.

DOI: 10.1002/acs

Note that—since we know in advance the type of isotope which has produced the impulse response—in Figure 8 the estimated parameters have been grouped according to the type of particle. This allows a direct understanding of the possibility to cluster the particles using the estimated parameters of the dynamic model.

By carefully inspecting Figure 8, it is apparent that, for each particle type, the spread of each estimated parameter is quite large. Moreover, for each parameter, the overlap of the estimated values for two different particles is quite large. This fact shows that a single parameter is not enough for a clear particle classification. The signature of a particle henceforth must be searched as a non-trivial non-linear combination of the four estimated parameters. The particle classification from the estimated parameters $\{\mu_s, \mu_f, \tau_s, \tau_f\}$ will be the topic of the next section.

4. LIGHT CHARGED PARTICLE CLASSIFICATION

As is well known, any isotope is univocally identified by its *charge*, given by its atomic number Z, and its mass, given by its atomic mass number A. The pair $\{A, Z\} \in \Re^2$ hence completely defines an isotope. LCP classification (the topic of this work) refers to low-charge and low-mass isotopes ($Z \leqslant 4$ and $A \leqslant 9$; particles which are out of this range will be simply classified as heavy ions).

The basic goal of this work is to classify the isotopes, starting from the measured (noisy) impulse responses detected by CHIMERA. The overall identification (classification) procedure hence can be viewed as an identification problem of the map from the whole impulse response $\{\tilde{v}(k)\}_{k=1,2,\ldots,1600} \in \Re^{1600}$ to the pair $\{A, Z\} \in \Re^2$.

The key idea of this work is to split this mapping into three main intermediate steps (see Figure 9, where the whole classification flow is described):

- The first step $\Re^{1600} \to \Re^4$ is performed via the state-space system identification of a second-order linear system characterized by four parameters $\{\mu_s, \mu_f, \tau_s, \tau_f\}$ from its impulse response; this step reduces the vector space $\Re^{1600}$ ($\{\tilde{v}(k)\}_{k=1,2,\ldots,1600} \in \Re^{1600}$) to the vector space $\Re^4$ ($\{\mu_s, \mu_f, \tau_s, \tau_f\} \in \Re^4$).
- The second step $\Re^4 \to \Re^2$ is performed via the supervised training of a standard non-linear parametric map; more specifically, a classical feed-forward multilayer perceptron neural network (NN) is used [25,29,30]; this step reduces the vector space $\Re^4$ ($\{\mu_s, \mu_f, \tau_s, \tau_f\} \in \Re^4$) to the vector space $\Re^2$ ($\{q_1, q_2\} \in \Re^2$). Note that $\{q_1, q_2\} \in \Re^2$ is simply the real-valued approximation of $\{A, Z\} \in \Re^2$.
- The third step $\Re^2 \to \Re^2$ is performed via a simple classification (threshold-based) map; this map is completely defined in Table II; this step reduces the vector space $\Re^2$ ($\{q_1, q_2\} \in \Re^2$) into the classification set ($\{A, Z\} \in \Re^2$).

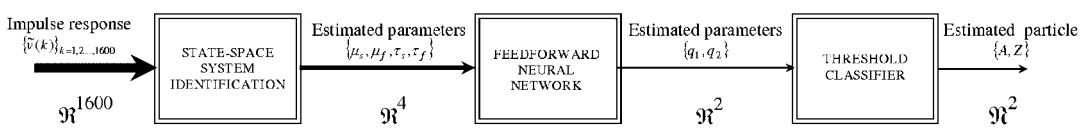

Figure 9. Classification flow.

DOI: 10.1002/acs

Table II. Classification table.

Threshold on q_1, q_2	Classification A, Z (isotope)
$q_1 \leqslant 1.5, q_2 \leqslant 1.5$	$A = 1, Z = 1$ (p)
$1.5 < q_1 \leqslant 2.5, q_2 \leqslant 1.5$	$A = 2, Z = 1$ (d)
$q_1 > 2.5, q_2 \leqslant 1.5$	$A = 3, Z = 1$ (t)
$q_1 \leqslant 3.5, 1.5 < q_2 \leqslant 2.5$	$A = 3, Z = 2$ (^{3}He)
$q_1 > 3.5, 1.5 < q_2 \leqslant 2.5$	$A = 4, Z = 2$ (α)
$q_1 \leqslant 6.5, 2.5 < q_2 \leqslant 3.5$	$A = 6, Z = 3$ (^{6}Li)
$q_1 > 6.5, 2.5 < q_2 \leqslant 3.5$	$A = 7, Z = 3$ (^{7}Li)
$q_1 \leqslant 8, 3.5 < q_2 \leqslant 4.5$	$A = 7, Z = 4$ (^{7}Be)
$q_1 > 8, 3.5 < q_2 \leqslant 4.5$	$A = 9, Z = 4$ (^{9}Be)
$q_1 > 9.5, q_2 > 4.5$	$A > 9, Z > 4$ (heavy ions)
$q_1 > 9.5, q_2 \leqslant 4.5$	Not classified

The first step (state-space system identification) has been extensively described in the previous section.

The feed-forward multilayer perceptron NN used in the second step is described by the following function:

$$q_l = \sum_{i=1}^{n_h} \alpha_{il} \tanh\left(\sum_{j=1}^{n_j} \beta_{ij}\theta_j + \gamma_i \right) \tag{8}$$

where the network output q_l, $l = 1, 2$ is the real-valued approximation of A and Z; θ_j, $j = 1, \ldots, n_j$ with $n_j = 4$ are the parameters estimated in the first step; $\alpha_{il}, \beta_{ij}, \gamma_i$, $i = 1, \ldots, n_h$, $l = 1, 2$, $j = 1, \ldots, n_j$ are the network parameters. The hidden layer is composed by $n_h = 10$ neurons. The training of the NN has been performed using a Levenberg–Marquardt minimization algorithm; this approach is very standard, well documented, and many off-the-shelf software packages can be used to this purpose.

The threshold-based classification table (Table II) is very simple: it reduces the real-valued NN output into an integer.

The whole identification and classification procedure has been applied to a subset of 7784 pulse responses. One thousand pulse responses, 100 for each isotope, have been kept out of the training set for validation purposes. The results of the whole classification procedure are condensed in Figures 10–12 and Table III. These results are obviously referred to the validation data set only.

Figure 10 shows the estimate of the atomic number Z provided by the NN (see also Table III, first column). Notice that the charge classification is very precise: only two beryllium particles are misclassified: one is classified as a heavy ion, one as a lithium ion.

A similar plot is shown in Figure 11 for the atomic mass number A (see also Table III, second column). Also in this case the classification is very precise, even if it is slightly worse than that of Z (in general, it is known that the charge estimation is easier than mass estimation).

In Figure 12 the above results are condensed on the (A, Z) plane for a complete particle classification (see also Table III, third column). Note that the overall particle classification is extremely precise.

DOI: 10.1002/acs

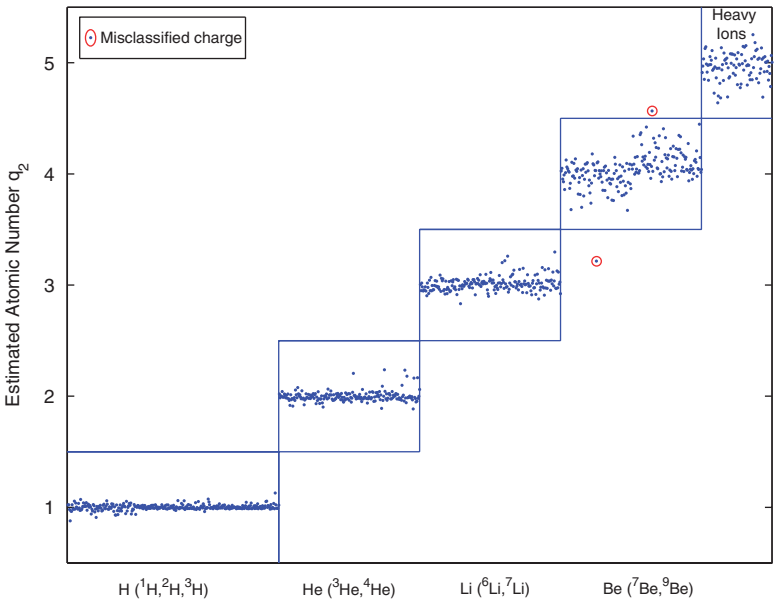

Figure 10. Classification results for the atomic number (charge).

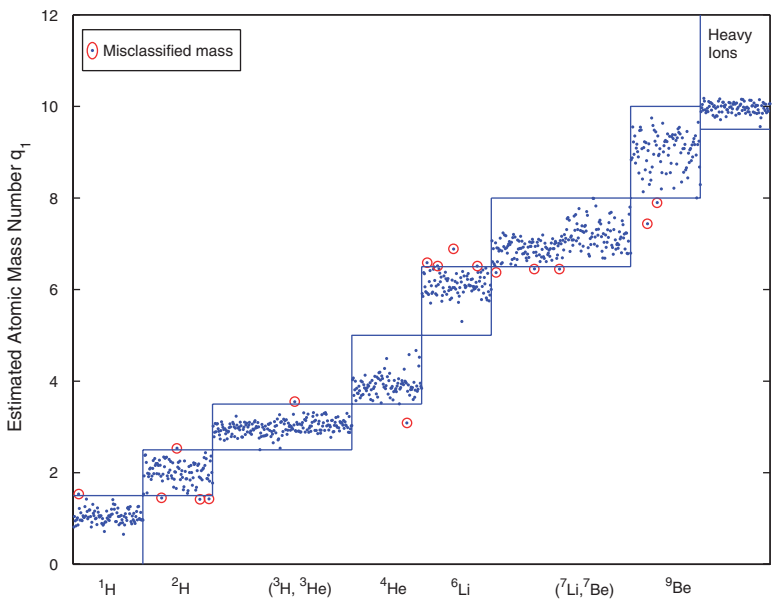

Figure 11. Classification results for the atomic mass number.

DOI: 10.1002/acs

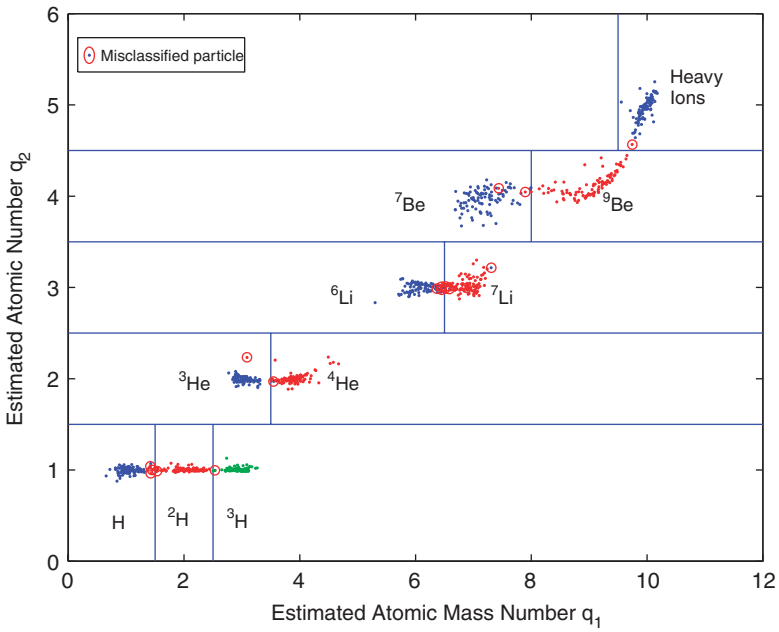

Figure 12. Classification results for the particle.

Table III. Condensed classification results on the validation data set.

Isotope	Correct estimation of Z (%)	Correct estimation of A (%)	Correct classification of the particle (%)
^{1}H (protons)	100	99	99
^{2}H (deuterons)	100	96	96
^{3}H (tritons)	100	100	100
^{3}He	100	99	99
^{4}He	100	99	99
^{6}Li	100	96	96
^{7}Li	100	97	97
^{7}Be	99	100	99
^{9}Be	99	98	97
Heavy ions	100	100	100

5. CONCLUSIONS

In this work, a complete procedure for the identification of light charged particles is proposed. The identification procedure is based on the analysis of the shape of the light pulses produced by nuclear isotopes during their interaction with the material of a scintillation detector. The main idea is to use the cascade of a state-space identification algorithm and a parametric non-linear map. The parametric non-linear map is fed with the parameters of the dynamic model.

The algorithm has been tested on a large set of impulse-responses.

DOI: 10.1002/acs

The whole procedure provides a very precise classification of the isotopes; moreover, it is fully automatic, i.e. there is no need for human operation in particle classification. This represents a significant advantage with respect to more classical classification techniques.

It is worth observing that the state-space algorithm provides an accurate estimation of the fast and the slow time constants of the impulse-responses, which are usually only roughly approximated. This is achieved by explicitly taking into account the preamplifier dynamics during the identification procedure.

Finally, notice that the present algorithm can be applied to any particle detection system based on scintillation detector light responses, provided that an adequate tuning procedure is performed to take into account the specific features of the considered detector.

ACKNOWLEDGEMENTS

This work has been supported by MIUR project, 'New methods for Identification and Adaptive Control for Industrial Systems'. Two of us (P.G. and L.Z.) want to thank CHIMERAPS collaboration for the precious help given in data collection.

REFERENCES

1. Aiello S, Anzalone A, Baldo M, Cardella G, Cavallaro S, De Filippo E, Di Pietro A, Feminò S, Figuera P, Guazzoni P, Iacono-Manno C, Lanzanò G, Lombardo U, Lo Nigro S, Musumarra A, Pagano A, Papa M, Pirrone S, Politi G, Porto F, Rapisarda A, Rizzo F, Sambataro S, Sperduto ML, Sutera C, Zetta L. Chimera: a project of a 4π detector of heavy ions reactions studies at intermediate energy. *Nuclear Physics A* 1995; **583**:461–464.
2. Alderighi M, Anzalone A, Baruzzi R, Cardella G, Cavallaro S, De Filippo E, Geraci E, Giustolisi F, Guazzoni P, Lanzalone G, Lanzano G, Pagano A, Papa M, Pirrone S, Politi G, Porto F, Russo S, Sechi G, Sperduto L, Zetta L. Processing CsI(Tl) 2-D matrices by means of neural networks and Markov random fields. *IEEE Transactions on Nuclear Science* 2002; **49**(4):1661–1668.
3. Aiello S, Anzalone A, Cardella G, Cavallaro S, De Filippo E, Di Pietro A, Feminò S, Geraci M, Guazzoni P, Iacono-Manno C, Lanzanò G, Lo Nigro S, Musumarra A, Pagano A, Papa M, Pirrone S, Politi G, Porto F, Rizzo F, Sambataro S, Sperduto ML, Sutera C, Zetta L. Light response and particle identification with large CsI(Tl) crystals coupled to photodiodes. *Nuclear Instruments and Methods in Physics Research A* 1996; **369**:50–54.
4. Alarja J, Dauchy A, Giorni A, Morand C, Pollaco E, Stassi P, Billerey R, Chambon B, Cheynis B, Drain D, Pastor C. Charged particles identification with a CsI(Tl) Scintillator. *Nuclear Instruments and Methods in Physics Research A* 1986; **242**:352–354.
5. Alderighi M, Anzalone A, Bassini R, Berceanu I, Blicharska J, Boiano C, Borderie B, Bougault R, Bruno M, Calí C, Cardella G, Cavallaro S, D'Agostino M, D'Andrea M, Dayras R, De Filippo E, Fichera F, Geraci E, Giustolisi F, Grzesczuk A, Guardone N, Guazzoni P, Guinet D, Iacono-Manno CM, Kowalski S, Laguidara E, Lanchais AL, Lanzalone G, Lanzanò G, Le Neindre N, Li S, Maiolino C, Majka Z, Manfredi G, Nicotra D, Paduszynski T, Pagano A, Papa M, Petrovici CM, Piasecki E, Pirrone S, Politi G, Pop A, Porto F, Rivet MF, Rosato E, Saccà G, Sechi G, Simion V, Sperduto ML, Steckmeier JC, Trifirò A, Trimarchi M, Urso S, Vannini G, Vigilante M, Wilczynski J, Wu H, Xiao Z, Zetta L, Zipper W. Particle identification method in the CsI(Tl) scintillator used for the CHIMERA 4 detector. *Nuclear Instruments and Methods in Physics Research A* 2002; **489**:257–265.
6. Benrachi F, Chambon B, Cheynis B, Drain D, Pastor C, Seghier D, Zaid K, Giorni A, Heuer D, LLeres A, Morandi C, Stassi P, Viano JB. Investigation of the performance of CsI(Tl) for charged particle identification by pulse-shape analysis. *Nuclear Instruments and Methods in Physics Research A* 1989; **281**:137–142.
7. Bingefors N *et al*. A novel technique for fast pulse-shaping using a slow amplifier at CERN. *Nuclear Instruments and Methods in Physics Research A* 1993; **236**:112–119.
8. Bittanti S, Gatti E, Ripamonti G, Savaresi SM. High accuracy fit of the poles of spectroscopy amplifiers designed for mixed analog-digital filtering. *IEEE Transactions on Nuclear Science* 1997; **44**(2):125–133.
9. Bittanti S, Gatti E, Ripamonti G, Savaresi SM. Poles identification of an analog filter for nuclear spectroscopy via subspace-based techniques. *IEEE Transactions on Control System Technology* 2000; **8**(1):127–137.
10. Georgiev A, Gast W. Digital pulse processing in high resolution high throughput gamma-ray spectroscopy. *IEEE Transactions on Nuclear Science* 1993; **40**(4):770–779.

DOI: 10.1002/acs

11. Laforest R, Ramakrishnan E, Rowland DJ, Delafield R, Guzman S, Ferro S, VAsal S, Winchester E, Yennello SJ. Particle identification with FAUST detector. *Nuclear Instruments and Methods in Physics Research A* 1998; **404**: 470–472.
12. Ripamonti G, Castoldi A, Gatti E. Multiple delay line shaping: a new class of weighting functions suitable for digital signal processing. *Nuclear Instruments and Methods in Physics Research A* 1994; **340**:584–593.
13. Skulki W, Momayezi M. Particle identification in CsI(Tl) using digital pulse shape analysis. *Nuclear Instruments and Methods in Physics Research A* 2001; **458**:759–771.
14. Storey RS, Jack W, Ward A. The fluorescent decay of CsI(Tl) for particles of different ionization density. *Proceedings of the Physical Society* 1958; **72**(463):1–8.
15. Ljung L. *System Identification*. Prentice-Hall: Upper Saddle River, NJ, 1999.
16. Lovera M. Subspace identification methods: theory and applications. *Ph.D. Thesis*, Politecnico di Milano, Milano, 1997.
17. Van Overschee P, de Moor B. N4SID: subspace algorithms for the identification of combined deterministic-stochastic systems. *Automatica* 1994; **30**(1):75–93.
18. Viberg M. Subspace methods in system identification. *Proceedings of IFAC Symposium on System Identification*, Copenhagen, 1994; 1–12.
19. Sjoberg J, Zhang Q, Ljung L, Benveniste A, Delyon B, Glorennec P, Hjalmarsson H, Juditsky A. Nonlinear black-box modeling in system identification: a unified overview. *Automatica* 1995; **31**(12):1691–1724.
20. Alderighi M, Anzalone A, Bassini R, Boiano C, Cardella G, Cavallaro S, De Filippo E, Geraci E, Giustolisi F, Guazzoni P, Laguidara E, Lanzalone G, Lanzanò G, Pagano A, Papa M, Pirrone S, Politi G, Porto F, Russo S, Sassi M, Sechi G, Zetta L. CHIMERA data acquisition via digital sampling technique. *IEEE Transactions on Nuclear Science* 2004; **51**(4):1475–1481.
21. Akimov YK. *Scintillation Counters in High Energy Physics*. Academic Press: London, 1965.
22. Birks JB. *Scintillation Counters*. Pergamon Press: London, 1960.
23. Ho B, Kalman RE. Efficient construction of linear state variable models from input/output functions. *Regelungstechnik* 1966; **14**:545–548.
24. Kung AM, Desai UB, Skelton RE. A generalized approach to q-Markov covariance equivalent realizations for discrete systems. *Automatica* 1988; **24**(4):507–515.
25. Liu K, Skelton R. Identification of linear systems from their pulse response. *Proceedings of American Control Conference* 1992; 1243–1247.
26. Zeiger H, McEwen A. Approximate linear realisations of given dimension via Ho's algorithm. *IEEE Transactions on Automatic Control* 1974; **19**(2):153.
27. Savaresi SM. Identification of hybrid filters for energy estimation in nuclear spectroscopy. *Internal Report No. 95.021*, Politecnico di Milano, 1995.
28. Golub GH, Van Loan CF. *Matrix Computations*. The John Hopkins University Press: Baltimore, MD, 1996.
29. Bittanti S, Picci G (eds). *Identification, Adaptation, Learning—The Science of Learning Models from Data*. Computer and Systems Sciences Series. Springer: Berlin, 1996.
30. Cybenko G. Approximation by superposition of a sigmoidal function. *Mathematics in Control Systems and Signals* 1989; **2**(4):303–314.

DOI: 10.1002/acs